DESIGN OF 4-CHANNEL POLYMER-BASED AWG DEMULTIPLEXER FOR DIRECT LASER WRITING LITHOGRAPHY

Dana Seyringer[1]*, Felix Wäger[1], Fadi Dohnal[1], Johann Zehetner[1], Peter Gaso[2], Dusan Pudis[2]

[1]Research Centre for Microtechnology, FHV - Vorarlberg University of Applied Sciences, Hochschulstr. 1, 6850, Dornbirn, Austria

[2]Department of Physics, Faculty of Electrical Engineering and Information Technology, University of Zilina, Zilina, Slovakia

Abstract

This study presents the design and simulation of a 4-channel polymer-based planar arrayed waveguide gratings optical demultiplexer for telecommunication applications. The demultiplexer was designed for a central wavelength of 1550 nm using the AWG-Parameters tool. A single-mode polymer waveguide structure with a 2 µm × 2 µm cross-section was employed, utilizing IP-Dip polymer as the core material and polydimethylsiloxane Sylgard 184 as the cladding. The AWG structure was designed and simulated using the PHASAR tool from Optiwave, while its transmission characteristics were analyzed with the AWG-Analyzer tool. Additionally, the optical properties and dimensions of the AWG structure were optimized to meet the manufacturing constraints of the direct laser writing lithography process. These optimizations are crucial for ensuring the scalability, performance, and practical fabrication of polymer-based photonic devices.

Keywords: *arrayed waveguide gratings, polymer-based AWG, direct laser writing, two-photon polymerization, photonics, telecommunication*

1. INTRODUCTION

Arrayed waveguide grating (AWG) is a planar waveguide structure widely employed in applications ranging from telecommunications [1], environmental monitoring [2] to biomedical diagnostics [3]. In optical communication networks, AWG-based multiplexers and demultiplexers enable high data throughput by facilitating wavelength division multiplexing (WDM), thereby significantly enhancing system capacity. In biomedical applications, AWGs serve as compact optical spectrometers in miniaturized, on-chip integrated optical systems for diagnostic techniques such as imaging and spectroscopy [4].

The performance of AWGs strongly relies on the waveguide structure whose optical properties are largely determined by the materials used. Depending on the application requirements, AWGs can be fabricated on various material platforms, including silica-on-silicon (SoS) waveguides [5], silicon-on-insulator (SOI) rib waveguides [6], buried InP/InGaAsP rib waveguides [7], polymer waveguides [8], and Si_3N_4 waveguides [9]. For telecommunication applications, the most suitable material platform is the so-called “low-index-contrast” platform using silica-on-silicon (SoS) or polymer waveguides. These waveguides are characterized by a low refractive index contrast between the waveguide core and cladding, and a large cross-sectional area. This results in low propagation losses and high coupling efficiency with optical fibers.

Direct laser writing (DLW) lithography, based on two-photon polymerization (TPP), is an advanced fabrication technique offering a cost-effective and rapid alternative to conventional planar technologies. The DLW offers fast prototyping of the polymer-based photonic devices such as waveguides, splitters or AWGs in two-dimensional (2D) or three-dimensional (3D) arrangement.

In this work, we present the design of a 4-channel AWG with various channel spacings, optimized to reduce the overall footprint of the structure to meet the fabrication constraints of the DLW lithography process. The most suitable AWG design will be fabricated in 2D arrangement using DLW, and the achieved results are evaluated and discussed.

2. AWG PRINCIPLE

An arrayed waveguide gratings consist of an array of waveguides (referred to as the phased array, PA) and two star couplers, as illustrated in Fig. 1a. One of the input waveguides launches the light containing multiple wavelengths (λ_1 to λ_n) into the input star coupler, which then distributes the light uniformly across the waveguide array. The light subsequently propagates through the PA waveguides to the output star coupler. The lengths of the PA waveguides are designed such that the optical path length difference (*dL*) between adjacent waveguides corresponds to an integer multiple of the central wavelength (λ_c) of the AWG demultiplexer. For this wavelength, the optical fields in the individual arrayed waveguides arrive at the input of the output star coupler with equal phase, thereby reconstructing the input field distribution at the entrance of the output coupler. Within the output star coupler, constructive interference causes the beam to converge at a specific focal point along the focal line in the image plane. Thus, for λ_c, the input field at the object plane of the input coupler is transferred to the center of the image plane of the output coupler. When the input wavelength shifts to $\lambda_c \pm \Delta\lambda$ (i.e., $\lambda_1, \lambda_2, ...$), a linear phase shift is introduced across the phased array. This results in a tilted phase front at the entrance of the output star coupler, causing the beam to focus at a different point in the image plane. By positioning output waveguides at these distinct focal points, the AWG spatially separates the different wavelengths, enabling wavelength demultiplexing [10]. Figure 1b presents the transmission spectrum, demonstrating four clearly separated optical signals.

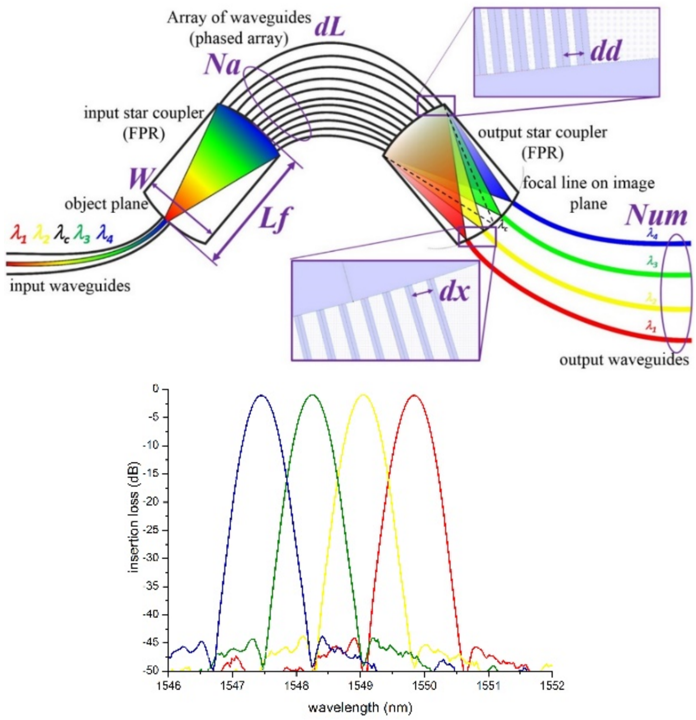

a) b)

Fig. 1. Principle of an AWG with the design parameters (a), transmission characteristics consisting of four separated optical signals (b) [11].

3. DESIGN

3.1. Design of waveguide structure

Various polymer waveguide structures were designed utilizing IP-Dip polymer as the core material and polydimethylsiloxane (PDMS) Sylgard 184 as the cladding to identify the technological limitations for single-mode operation at a wavelength of λ_c = 1550 nm. To minimize polarization- and wavelengthdependent losses, a square cross-section was selected for the waveguide geometry. Figure 2a shows the cross-section of the designed waveguide structure, including the key design parameters: the width and height of the waveguide (*w*), as well as the refractive indices of the core (n_c = 1.53) and the cladding (n_{cl} = 1.3997). Based on simulation results, the final dimensions of the waveguide were set to 2 µm × 2 µm. Figure 2b shows the simulated field distribution in the designed waveguide showing the single-mode operation.

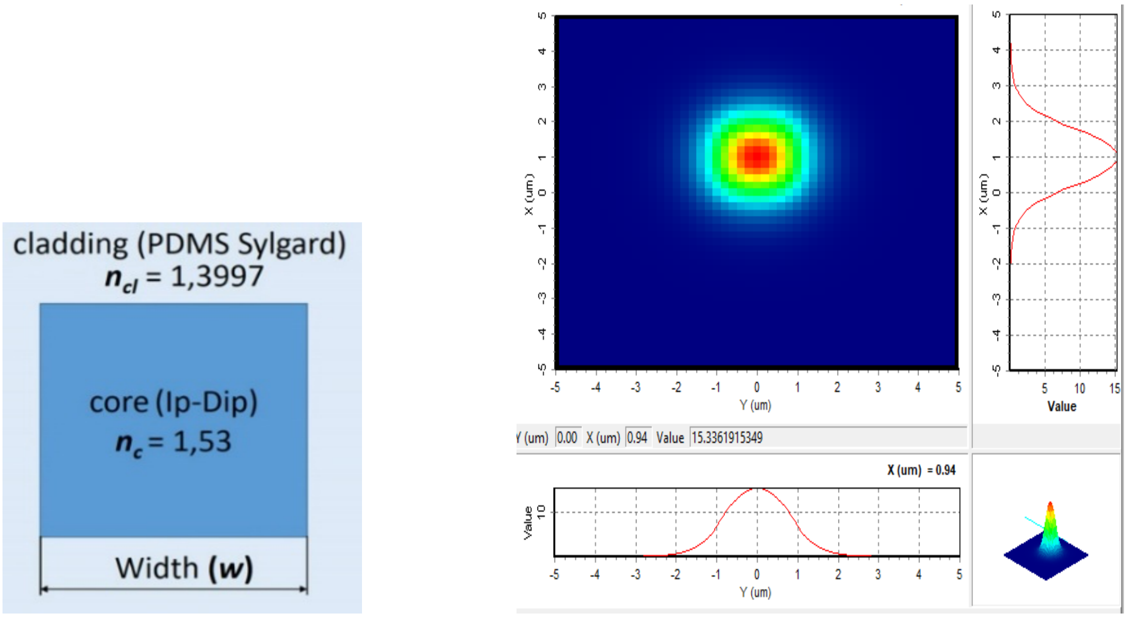

a) b)

Fig. 2. Cross-section of the used polymer waveguide structure (a); Simulated field distribution showing the single-mode operation. (b).

3.2. Design of AWG structure

In the first step, the 4-channel, 100-GHz AWG structure was designed. For the calculation of AWG design parameters, which are essential to create the AWG layout, the in-house developed tool “AWG-Parameters” was used [11]. Figure 3 shows the user interface of the tool.

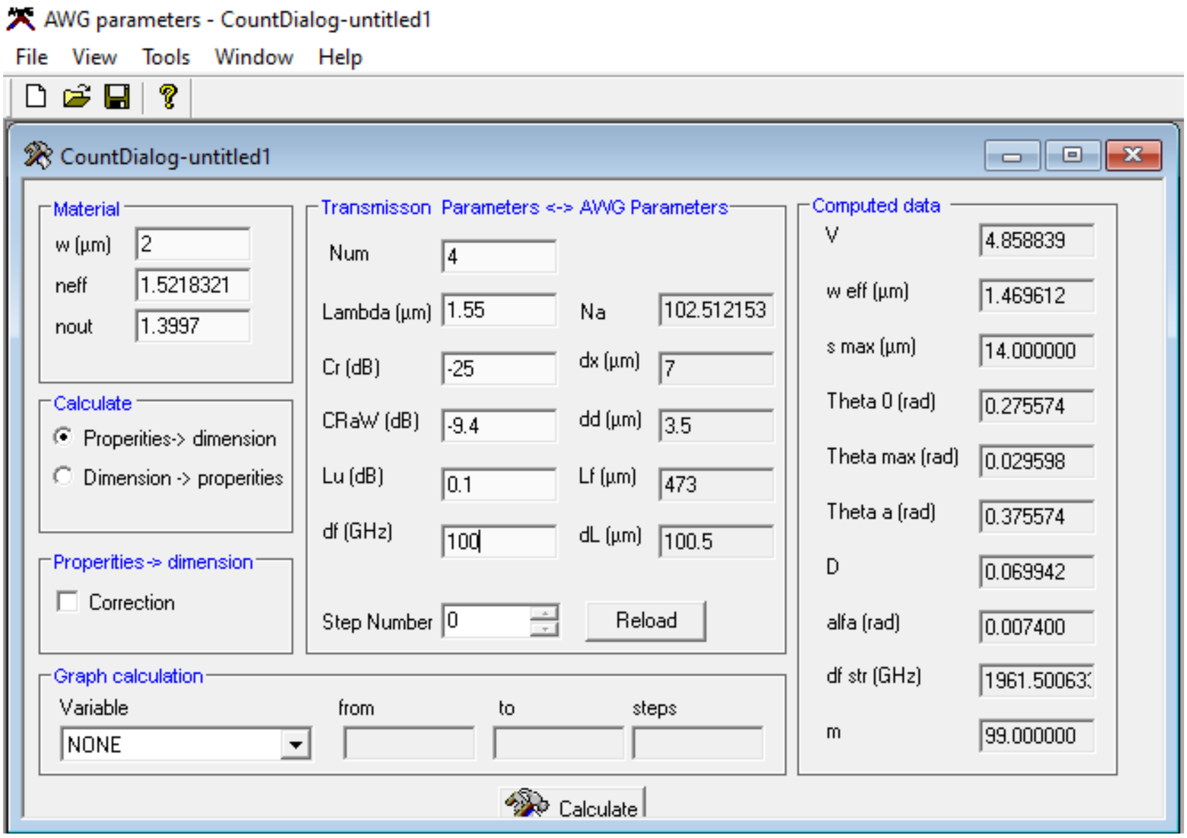

Fig. 3. User interface of the AWG-Parameters tool calculating input design parameters [11].

AWG design parameters are as follows (graphical representations of these parameters are in Fig.1):

- waveguide separation between PA waveguides (parameter *dd*),
- waveguide separation between input/output waveguides (parameter *dx*),
- length of the star coupler (parameter *Lf*),
- optical path length difference between adjacent waveguides in the phased array (parameter *dL*),
- number of array waveguides, *Na* is usually calculated from the width of the input star coupler, *W* divided by the waveguide separation between PA waveguides (*Na* ~ *W*/*dd*).

3.3. Simulation of AWG structure

AWG design parameters from the AWG-Parameters tool serve as input for commercial photonic design tools to generate the AWG layout. Figure 4 shows the layout of the designed 4-channel, 100-GHz AWG created using the commercial PHASAR tool from Optiwave [12]. The output from the simulations are the transmission characteristics.

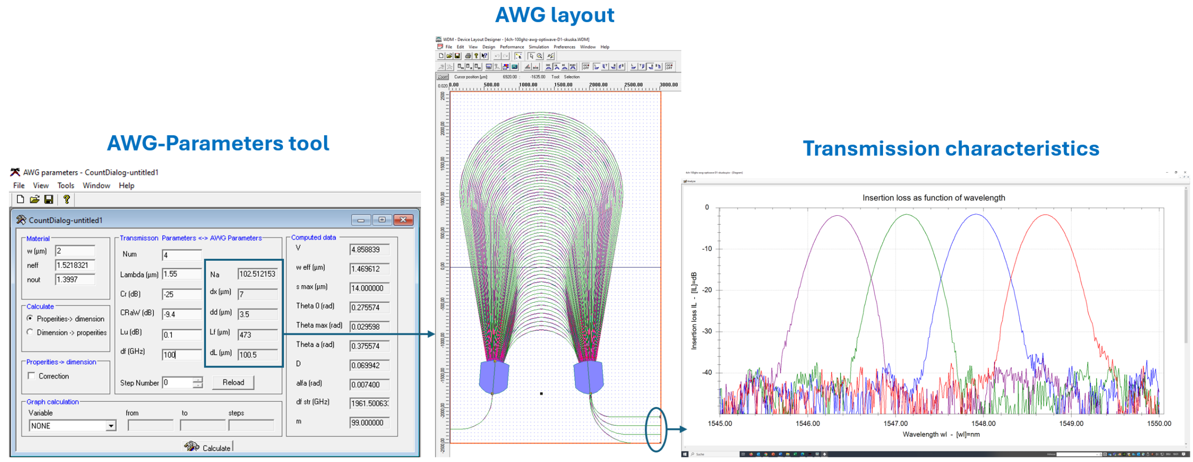

Fig. 4. Layout of the designed 4-channel, 100-GHz polymer-based AWG created using the PHASAR tool from Optiwave with simulated transmission characteristics.

3.4. Analysis of transmission characteristics

The AWG-Analyzer tool [11] was used to extract key transmission parameters from the simulated transmission spectra of the designed AWGs. Figure 5 shows the graphical user interface of the tool. The simulated data obtained from the PHASAR tool are displayed in the "Raw-Data" window, while the corresponding graphical representation is shown in the "Diagram" window. A total of nineteen transmission performance parameters are computed and listed in the "AWG Transmission Parameters" window. The definitions and detailed descriptions of these parameters can be found in [11].

The most important parameters are:

- Peak insertion loss, *pIL* = –1.903 dB
- Insertion loss, *IL* = –2.832 dB
- Peak insertion loss uniformity, *pILu* = 0.323 dB
- Insertion loss uniformity, *ILu* = 0.367 dB
- Adjacent channel crosstalk, *AX* = 32.618 dB
- Non-adjacent channel crosstalk, *nAX* = 33.531 dB
- Background crosstalk, *BX* = –42.615 dB

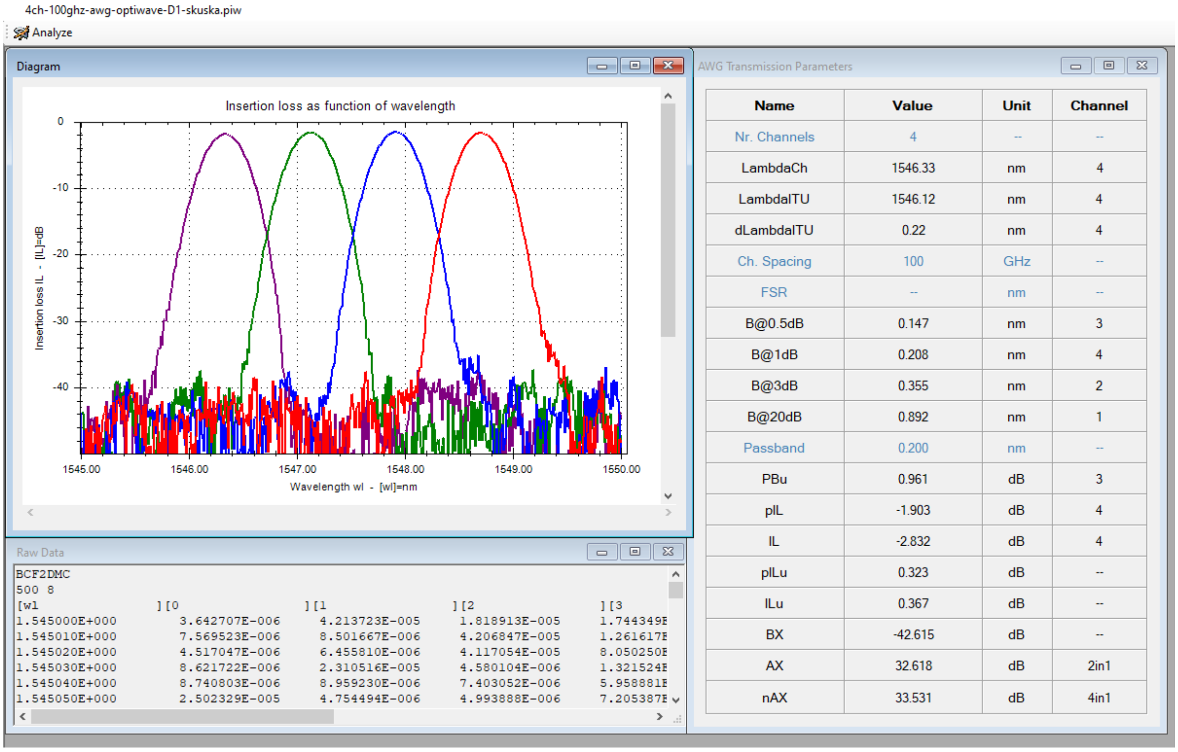

Fig. 5. User interface of the AWG-Analyzer tool [11].

4. AWG OPTIMISATION

As shown in Fig. 5, the calculated transmission parameters indicate outstanding AWG performance, including low insertion loss (*IL, pIL*), low non-uniformity across all output channels *(ILu, pILu*), and high channel isolation (*AX, nAX, BX*). However, the footprint of the AWG structure depicted in Fig. 4 is 2.6 mm × 4.8 mm, which exceeds the practical limits of the DLW fabrication process. Analysis of the AWG layout reveals that the phased array waveguides occupy the largest portion of the overall structure. To reduce the physical size of this region without performing a complete redesign, the channel spacing can be increased from 100 GHz to 200 GHz. By doubling the channel spacing while keeping all other design parameters constant, the size of the phased array can be approximately halved.

Figure 6 compares three different AWG configurations: a 4-channel AWG with 100 GHz channel spacing (referred to as Design-1), a 4-channel AWG with 200 GHz spacing (Design-2), and a 4-channel AWG with 400 GHz spacing (Design-3). All three AWGs have the same design parameters except parameter *dL* and also the same standard liner tapers. As can be seen, the 200 GHz design achieved a reduced footprint of 1.8 mm × 2.8 mm, while the 400 GHz design further decreased the size to 1.4 mm × 1.9 mm.

4.1. Further optimisation

Further size reduction of the 4-channel, 400-GHz AWG (Design-3) focused on lowering the number of waveguides in the phased array, *Na*. As previously mentioned, *Na* is typically determined by the width *W* of the input star coupler divided by the waveguide separation, *dd* in the phased array. However, to maintain low channel crosstalk the width of the coupler*, W* must not be smaller than the width of the far-field intensity distribution at the output aperture of the input star coupler [10]. This implies that if the far-field intensity profile can be shaped to be narrower, the number of phased array waveguides can be reduced without degrading AWG performance. Based on this principle, we investigated the use of different input tapers positioned in front of the input star coupler to reshape the far-field profile and evaluated their effect on the AWG performance.

Figure 7 shows three variants of the 4-channel, 400-GHz AWG structure (Design-3), each incorporating a different taper design. These modifications enabled a further reduction in the number of PA waveguides and consequently a smaller overall device footprint: Design-3a achieved a size of 1.3 mm × 1.75 mm, Design-3b reached 1.25 mm × 1.6 mm, and Design-3c was reduced to 1.0 mm × 1.4 mm.

Design-1 Design-2 Design-3

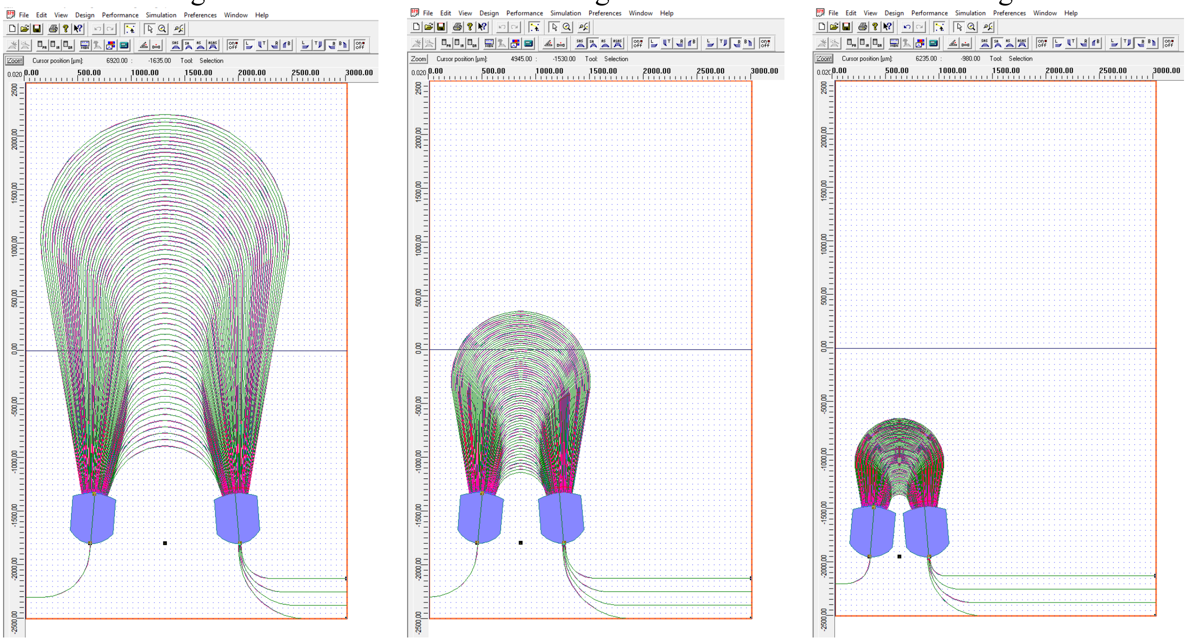

Fig. 6. Comparison of a 4-channel, 100-GHz AWG, a 4-channel, 200-GHz AWG and finally a 4-channel, 400-GHz AWG structures.

Design-3a Design -3b Design-3c

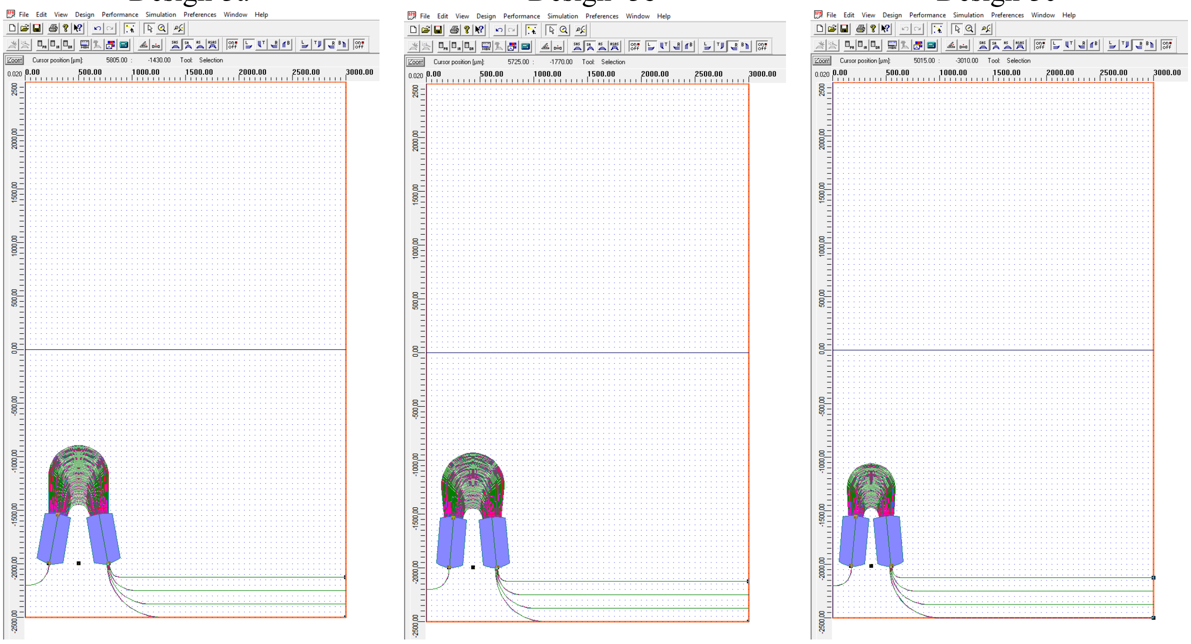

Fig. 7. Comparison of a 4-channel, 400-GHz AWGs with different input tapers.

5. DISCUSSION

Figure 8 presents a comparison of the transmission characteristics for Design-1, Design-3, Design-3a, and Design-3c. In all designs, the four transmitted optical channels are clearly separated. However, the implementation of different input taper geometries affects the spectral shape of the transmitted signals and thus impacts overall AWG performance. Design-1 and Design-3 exhibit typical Gaussian-shaped transmission spectra, characterized by low insertion loss and high channel isolation. In contrast, Design-3a shows a slightly semi-flat-top profile, while Design-3c demonstrates an almost flat-top shape. These flatter spectral responses result in an increased insertion loss and elevated channel crosstalk compared to the Gaussian-shaped designs but on the other hand feature much better detection conditions (i.e., higher tolerance to laser wavelength deviations from the given channel center wavelength) [13].

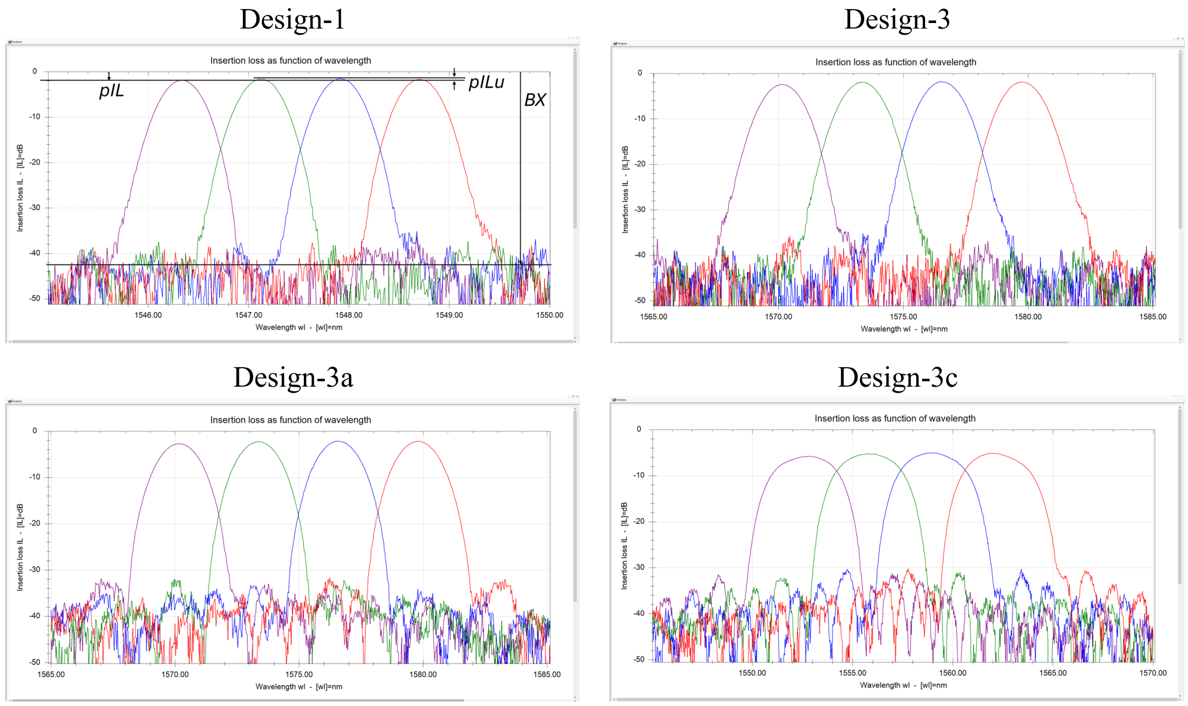

Fig. 8. Comparison of transmission characteristics of a 4-channel, 100-GHz AWG (Design-1), a 4-channel, 400-GHz AWG (Design-3) and optimized 4-channel, 400-GHz AWGs with different input tapers (Design-3a and 3c).

Table 1 provides a summary of the calculated transmission parameters for all AWG designs, confirming their respective performance characteristics.

AWG	Design-1	Design-2	Design-3	Design-3a	Design-3b	Design-3c
pIL	–1.903	–2.062	–2.462	–2.745	–4.32	–5.825
IL	–2.832	–3.015	–3.383	–3.538	–5.285	–6.158
pILu	0.323	0.294	0.631	0.535	0.664	0.776
ILu	0.367	0.363	0.624	0.557	0.832	0.905
AX	32.618	32.905	32.264	28.572	26.98	19.207
nAX	33.531	34.082	34.667	31.748	28.55	28.723
BX	–42.615	–44	–45.14	–41	–41.6	–41.189

Table 1. Transmission parameters from all AWG designs calculated by the AWG-Analyzer tool.

6. CONCLUSION

We have presented the design and optimization of polymer-based 4-channel AWGs intended for fabrication using direct laser writing lithography, which enables rapid prototyping of photonic waveguide devices in both 2D and 3D configurations. The AWGs were designed as planar waveguide structures with different channel spacings to minimize the overall footprint. Further size optimization was achieved by implementing different input taper geometries. The simulated transmission characteristics and the calculated performance parameters confirm the effectiveness of the proposed designs. In the next phase, fabrication of the AWG prototypes using the DLW technique is planned.

ACKNOWLEDGMENTS

This work was carried out under project No. 2024-10-15-002 (POLY-MUX), SAIA, n. o., Aktion Österreich – Slowakei.

REFERENCES

1. Uetsuka, H. 2004, "AWG technologies for dense WDM applications," in *IEEE Journal of Selected Topics in Quantum Electronics*, vol. 10, no. 2, pp. 393-402, March-April 2004, doi: 10.1109/JSTQE.2004.827841.
2. Zehetner, J., Seyringer, D., Dohnal, F., Serecunova, S., Seyringer, H., Hotovy, I., Rehacek, V. 2024, “AWG-spectrometer to analyze absorption spectra of optical gas sensors fabricated by femtosecond laser processing”, *AIP Conf. Proc.* 3054, 080003, https://doi.org/10.1063/5.0188211.
3. Agneter, A., Muellner, P., Nguyen, Q., Seyringer, D., et al. 2024, “CMOS optoelectronic spectrometer based on photonic integrated circuit for in vivo 3D optical coherence tomography”, *PhotoniX 5, 31,* https://doi.org/10.1186/s43074-024-00150-7.
4. Bradshaw, J. T., Mendes, S. B. and Saavedra, S. S. 2005, “Planar integrated optical waveguide spectroscopy,” *Anal. Chem.* 77, 28A–36A, https://doi.org/10.1021/AC053303Q.
5. Okamoto, K. 2012, “Progress and technical challenge for planar waveguide devices: silica and silicon waveguides,” *Laser Photonics Rev*. 6, 14–23, https://doi.org/10.1002/lpor.201100003.
6. Cheung, T. S., et al. 2021, “Low-loss and high contrast silicon-on-insulator (SOI) arrayed waveguide grating”, *Proc. Conf. Lasers Electro-Optics*, pp. 1–2, https://doi.org/10.1364/CLEO_SI.2012.CM4A.5.
7. Soares, F.M., et al. 2010, “Monolithically integrated InP wafer-scale 100-channel times 10-GHz AWG and Michelson interferometers for 1-THz-bandwidth optical arbitrary waveform generation”, *Proc. 2010 Conf. Optical Fiber Communication, Collocated National Fiber Optic Engineers Conf.*, pp. 1–3.
8. Bo, Y., et al. 2011, “Compact arrayed waveguide grating devices based on small SU-8 strip waveguides”, *J. Lightwave Technol.* 29 (13), 2009–2014, 10.1109/JLT.2011.2157302.
9. Martens, D., et al. 2015, “Compact silicon nitride arrayed waveguide gratings for very near-infrared wavelengths”, *IEEE Photonics Technol. Lett*., 27, 137–140, 10.1109/LPT.2014.2363298.
10. Smit, M.K., et al. 1996, “PHASAR-based WDM-devices: principles, design and applications”, *J. Sel. Top. Quantum Electron.*, 2, 236–250, 10.1109/2944.577370.
11. Seyringer, D.,2016, “Arrayed waveguide gratings”, *SPIE Spotlights*, Volume: SL16, Bellingham, Wash., 2016, ISBN 978-1-5106-0359-2.
12. Optical Wavelength Division Multiplexing <https://optiwave.com/resources/wdm-phasar-download/> (March 2025).

13. Maru, K. and Abe, Y. 2007, “Low-loss, flat-passband and athermal arrayed-waveguide grating multi/ demultiplexer”, *Opt. Express* 15(26), 18351–18356, https://doi.org/10.1364/OE.15.018351.